Macromolecules

ARTICLE

pubs.acs.org/Macromolecules

Thermoreversible Gelation of Poly(vinylidene fluoride-*co*-chlorotrifluoroethylene): Structure, Morphology, Thermodynamics, and Theoretical Prediction

P. Jaya Prakash Yadav,[†,§] Biswajit Maiti,[‡] B. K. Ghorai,[§] P.U. Sastry,[⊥] A.K. Patra,[⊥] Vinod K. Aswal,[⊥] and Pralay Maiti*[,†]

[†]School of Materials Science and Technology, Institute of Technology, Banaras Hindu University, Varanasi 221 005, India

[‡]Department of Chemistry, Banaras Hindu University, Varanasi 221005, India

[§]Department of Chemistry, Bengal Engineering and Science University, Shibpur, Howrah 711 103, India

[⊥]Solid State Physics Division, Bhabha Atomic Research Centre, Trombay, Mumbai 400 085, India

ABSTRACT: Thermoreversible gelation of a copolymer, poly(vinylidene fluoride-*co*-chlorotrifluoroethylene), has been studied in a series of aromatic diesters (phthalates) with varying aliphatic chain length, *n*. The gelation rate gradually increases with increasing *n*, but no gelation occurs in dioctyl phthalate (*n* = 8), giving rise to a solvent dependency. Structures of gels and dried gels have been studied through X-ray diffraction and FTIR studies. Fibrillar morphology is evident for the series of solvents, but its dimension (both lateral and diameter) systematically changes with *n*. Solvent retention power of gels has gradually been increased with increasing *n* while the thermal degradation of copolymer occurs at same temperature, reflecting varying interactions between copolymer and various aliphatic chain length phthalates in gels. Phase diagrams of the gels exhibit the formation of two kinds of polymer−solvent complexes and have been predicted theoretically through electronic structure calculation. Both the small-angle neutron scattering (SANS) and small-angle X-ray scattering (SAXS) have been performed to elucidate the structure of fibril indicating gradual changes in lamellar organization. The experimental data have been fitted with different models and power law to check their validity. Molecular modeling has been carried out to understand the nature of interaction between copolymer and the solvent through energy minimization program and found a typical *n* = 6 value of lowest dipolar distance, indicating strongest interaction. The magic number of six has further been explored through quantum chemical calculations.

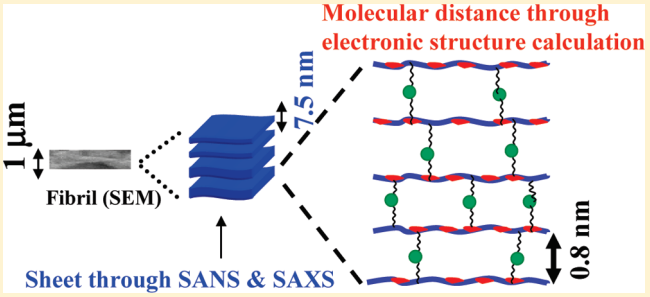

INTRODUCTION

Fluoropolymers have many interesting properties including piezo- and pyroelectric properties, and at the same time they form gels in various organic solvents and can be used as gel electrolytes in membranes and batteries. Fluoropolymers have required mechanical, thermal, and chemical stabilities for practical applications as well. Thermoreversible polymer gels are of potential interest for the development of new design lithium ion batteries.[1−3] Among the various polymers that can be used for this purpose are poly(vinylidene fluoride) (PVDF) and its various copolymers. PVDF and its copolymers have intensely been studied because of their interesting structure, microstructure, and electronic properties.[4−9] There are many reports on PVDF and some of its copolymer gelation, its mechanism, structure, morphological, thermal, and mechanical properties in different solvents like aliphatic diesters with varying intermittent chain length, aromatic diesters, and cyclic ketones.[10−20] Many groups have been studied polymer−solvent compound formation from thermodynamic investigations.[20−24] Recently, we have reported thermoreversible gelation on PVDF copolymer, i.e., poly(vinylidene fluoride-*co*-hexafluoropropylene), in aromatic diesteres (phthalates) [$Ph(COOC_nH_{n+1})_2$].[19] Gel has some definite capability to retain solvents in the network structure, and solvent retention power has been studied for pure PVDF in our earlier work[18] and other polymers[25] using thermogravimetric techniques. Small-angle neutron scattering and small-angle X-ray scatterings are powerful techniques to study the structure, mass, and surface fractals and morphology of gels.[26−32] Usually, a power-law behavior ($I \sim q^{-D}$) follows for most of the gels and dried gels.[18,19] Small-angle neutron scattering data can be fitted with the existing model to check the validity of different models. Another important aspect of prediction of experimental results theoretically by means of energy minimization program, and there are only a few reports in the literature including our previous results on other systems.[17,19,33]

Copolymer of vinylidene fluoride with chlorotrifluoroethylene P(VDF-*co*-CTFE) is an interesting polymer and are widely used

Received: February 7, 2011
Revised: March 13, 2011
Published: March 28, 2011

Scheme 1. (a) Chemical Formula of CTFE Copolymer and (b) Possible Interaction Sites between Polymer and Solvent Molecules through Dipole

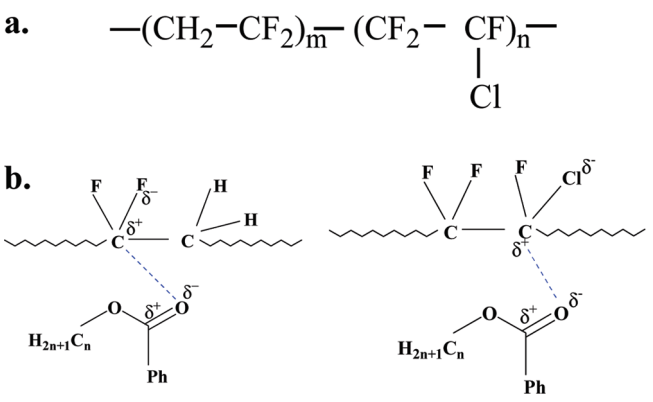

in the electrolyte membranes. Unfortunately, there is no study of its gelation behavior in organic solvents. In this paper, we are reporting the gelation kinetics, structure, solvent retention, and morphological behavior of its gel. Thermodynamic study and polymer−solvent complexation in gels have been investigated for P(VDF-*co*-CTFE) in different aromatic diesters. Structural details of the fibrils have been carried out through small-angle neutron scattering and small-angle X-ray scattering studies. The central theme of this work is to study the changes in gelation behavior in phthalates with varying aliphatic chain lengths.[34−36] The gelation behavior and its mechanism have been predicted theoretically by using electronic structure calculation. A schematic model has been given to the formation of fibillar structure starting from molecular self-assembly to fibrils through lamellar organization.

EXPERIMENTAL SECTION

Materials and Methods. We have used commercial poly(vinylidene fluoride-*co*-chlorotrifluoroethylene) copolymer (Scheme 1) (SOLEF 31008), Ausimont, Italy, of MFI 24 g/10 min (230 °C, 5 kg). Henceforth, we will term the copolymer as CTFE. The solvents used in the work, dimethyl phthalate (DMP) and diethyl phthalate (DEP) from Loba Chieme and dibutyl phthalate (DBP) from Merck, were used as received. For the preparation of gel, a predetermined amount of polymer was dissolved in weighed amount of solvent (phthalate) at 200 °C to make a homogeneous solution. The homogeneous solution has been transferred to predetermined temperature bath and check the time until it freezes. The time of seization of flow was taken as gelation time. Dried gels were prepared by host−guest solvent to replace the phthalates.[17−19] CTFE-phthalate gel had been taken in the Petri dish immersed with low boiling solvent (cyclohexene) at room temperature for 12 h followed by its decantation, and this process was repeated with fresh cyclohexene every 12 h for a week to complete removal of phthalates from the gels. The resulting gels were initially dried at room temperature followed by under reduced pressure at ambient temperature for 3 days to keep the morphology intact.

Gelation Kinetics. Gelation kinetics was studied by test tube tilting method of CTFE gels with a concentration range of 4−20% (w/v). Gelation kinetics is measured as a function of polymer concentration and temperature. Gels were prepared in the test tube at 200 °C temperature quickly transferred into the constant temperature bath and kept there until it fridge. Gelation time was measured where there is no flow occur after tilting the test tube. Gelation rate is defined as the reciprocal of gelation time.

X-ray Diffraction (XRD). X-ray diffraction experiments were performed using a Philips wide-angle X-ray diffractometer (DS-7) with Cu Kα radiation and a graphite monochromator (wavelength, $\lambda = 0.154$ nm). CTFE dried gels were scanned at 2°/ min of diffraction angle 2θ from 10° to 40°.

FTIR Spectra. FTIR spectra of dried samples were taken in transmittance mode at a wavenumber range of 1000−400 cm^{-1}. CTFE dried gels powder mixed in KBr were used for FTIR measurements. FTIR studies were performed on a Nicolet 5700 instrument with the resolution of 4 cm^{-1} taking 200 scans.

Morphology. The CTFE dried gels morphology was examined by using Zeiss SEM instrument operated at 10 kV. Samples were coated with gold−palladium by means of a sputtering apparatus before observation.

Thermal Decomposition. Thermal decompositions of CTFE gels (10% (w/v)) were examined by using thermogravimetric analysis (TGA) (Mettler-Toledo) fitted with the differential thermal analyzer (DTA). All the experiments were performed using the heating rate of 10 °C min^{-1} in a nitrogen atmosphere. Thermal studies have been performed to determine the solvent retention and degradation behavior of CTFE-phthalate gels.

Differential Scanning Calorimetry (DSC). CTFE gel samples were scanned at the heating rate of 10 °C/min. The peak temperature and the enthalpies of fusion were measured using the computer attached with the instrument. After the first melting, the gels were cooled down at a constant rate of 10 °C/min to find the gelation temperature, and the heats of gelation were measured in a similar manner. A Mettler 832 DSC was used for the experiments, and it was calibrated with indium and zinc before use.

Small-Angle Neutron Scattering. Small-angle neutron scattering of CTFE dried gels were performed on the spectrometer at the Dhruva reactor at Bhaba Atomic Research Centre, Mumbai, India. The data of the dried gels were collected in the scattering wavevector (q) range of 0.17 $nm^{-1} \leq q \leq 3.5$ nm^{-1}. The data were corrected for the background contributions and incoherent scattering which originates due to hydrogen atoms in the sample.

Small-Angle X-ray Scattering. Small-angle X-ray (SAXS) measurements were carried out using a Rigaku small-angle goniometer mounted on rotating anode X-ray generator (Cu Kα). Scattered X-ray intensity $I(q)$ was recorded using a scintillation counter with pulse height analyzer by varying the scattering angle 2θ, where q is the scattering vector given by $4\pi \sin(\theta)/\lambda$ and λ is the wavelength of incident X-rays. Data were recorded on three samples, namely DMP, DEP, and DBP derived dried gels. The intensities were corrected for sample absorption and smearing effects of collimating slits.[31]

Modeling. Molecular modeling has been carried out through energy minimization program to understand the intermolecular interactions involved between α-CTFE and phthalates with various aliphatic chain lengths using the AM1 method, as implicated in Chem3D Ultra 7.0. The dipole−dipole interactions computed between ⟩C═O groups of phthalate and ⟩CF_2 and ⟩$CF_2CF(Cl)$ groups of CTFE. We have modeled CTFE as a truncated chain consisting of minimum 12 monomer units (considering alternating vinylidene fluoride and chlorotrifluoroethylene).

To get insight into the magic number $n = 6$ for gelation, we have computed charge separation of ⟩C═O group with varying n values from 1 to 9 through quantum chemical calculations. For relatively large molecular systems, the density functional theory (DFT) is found to be an efficient method. These calculations were performed using a hybrid version of DFT and Hartree−Fock (HF) methods, namely, B3LYP density functional theory method in which the exchange energy from Becke's exchange functional is combined with the exact energy from Hartree−Fock theory. Along with the component exchange and correlation functionals, three parameters define the hybrid functional, specifying

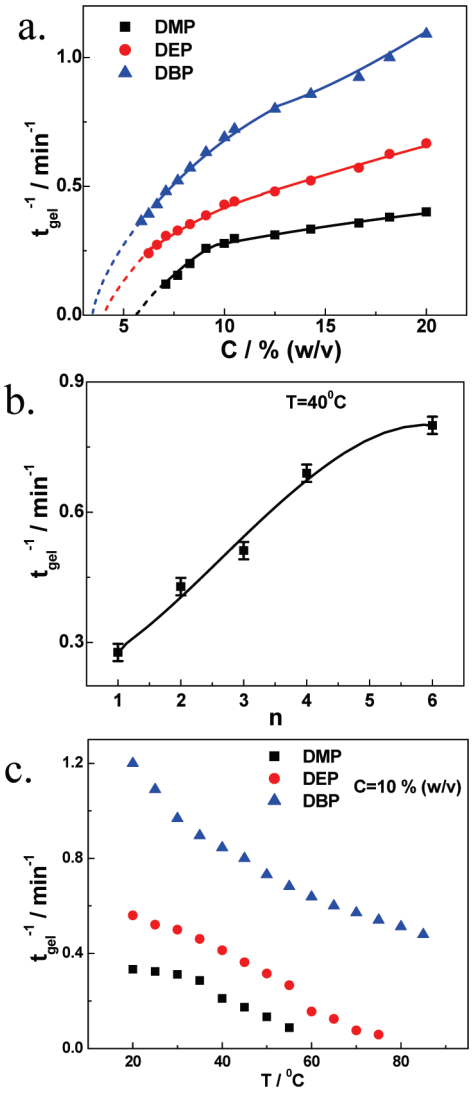

Figure 1. Gelation rate versus (a) concentration at 40 °C, (b) *n*, aliphatic chain length, and (c) temperature for 10% (w/v) of CTFE in (■) DMP, (●) DEP, and (▲) DBP.

how much of the exact exchange is mixed in. Although the three semi-empirical parameters are optimized primarily to reproduce thermochemistry of small organic molecules, it has been proven to perform exceptionally well for relatively larger organic molecules. The geometry of phthalate molecules was optimized at the B3LYP/6-31G(d,p) level of theory. All the calculations were performed using Gaussian 03 suits of program.[39]

■ RESULTS AND DISCUSSION

Gelation Kinetics. The gelation rates (t_{gel}^{-1}) have been measured at three different phthalates at 40 °C as a function of polymer concentration (Figure 1a). The gelation rates are in the order of DMP < DEP < DBP and increases systematically with increasing the aliphatic chain length (*n*) of diester (phthalates) for the entire concentration range studied here, indicating greater interaction for higher *n* phthalates with CTFE copolymer. This trend is similar to the gelation rate of pure PVDF, but the absolute of t_{gel}^{-1} value is little less in copolymer (CTFE) as compared to pure PVDF.[17] CTFE does not form gel in dioctyl phthalate (DOP; $n = 8$), and instead the polymer phase separates macroscopically as a result of the formation of bigger crystallites. Gelation rate is related to interacting nature between polymer and solvent leading to compound formation. It is noteworthy to mention that simultaneous interactions between polymer−polymer and polymer−solvent are equally important, and the polymer−polymer interaction is stronger in DMP, a relatively poor solvent, whereas the polymer−solvent interaction becomes increasingly dominating over the polymer−polymer interaction at higher homologues of phthalates, comparatively good solvent. The gelation rates have been plotted in Figure 1b to indicate the relative rates at a particular concentration (10% (w/v)) as a function of aliphatic chain length (*n*) showing obvious increase of t_{gel}^{-1} for CTFE copolymer with higher *n*. Moreover, the gelation rate decreases with decreasing CTFE concentration, and the extrapolation of the curves to $t_{gel}^{-1} \rightarrow 0$ provides critical gelation concentration, c_g^*, a thermodynamic parameter below which gelation cannot occur because of critical molecular cluster size required for compound formation, a necessary step for gelation. The c_g^* are 5.8, 4.0 and 3.5% (w/v) for DMP, DEP, and DBP, respectively, showing decreasing order for higher *n* phthalates. Here again, the relative value of c_g^* is slightly higher as compared to pure PVDF (4.0, 3.5 and 2.9% (w/v) for DMP, DEP, and DBP, respectively) in the same set of solvents. Sol-to-gel transformation is a two-step process: first, several microgel clusters were uniformly formed, and later these microclusters progressively got connected together by polymer chains to form a three-dimensional network. At fixed concentration of polymer (10% w/v), gelation rate decreases with increasing temperature (Figure 1c), but the relative rate of gelation is the same as discussed earlier for various phthalates. Initially, the microgels are formed in every solvent whose motion obviously increases with increasing temperature. Slower connectivity of the microgels as a result of greater motion is expected at high temperature, causing lower gelation rate. Another reason might be due to slower crystallization rate at higher temperature which eventually retards the gelation phenomena at higher temperature.

Structure. PVDF and its copolymers, having three modes of molecular conformations, TGTḠ, TTTT, and TTTGTTTḠ, crystallize in four different types of crystalline forms distinguished as α, *β*, *γ*, and *δ* forms.[40] The α phase (TGTḠ) is inactive with respect to piezo- and pyroelectric properties while the *β*-form (all trans) exhibits ferroelectric activity, suitable for electroacoustic transducer applications.[41] Usually PVDF and its copolymers crystallizes in α-phase, appearing peak positions at $2\theta = 17.6°$, 18.3°, and 19.9° corresponding to (100), (020), and (110) planes, respectively.[42] Figure 2a shows the crystalline structure of dried gels in all three solvents, and it is clear that the α-crystalline form is predominant.[17] Moreover, the higher crystallinity of dried gel is apparent for higher homologue of phthalates as manifested from the stronger XRD peaks for higher *n* phthalates. Higher heats of fusion for higher *n* phthalates further clarify the issue and will be discussed in thermal behavior section in detail. The XRD patterns of gels, in the presence of solvent, have been presented in Figure 2b. Interestingly, there are two additional peaks at 14.2° and 21.8° in addition to the normal α-crystalline form shown in Figure 2a. The extra peak at 21.8° in gel samples is presumably due to polymer−solvent complexes which disappear after removing the solvent from the gel in dried gels. The peak at 14.2° is primarily due to the amorphous halo which gradually becomes less intense with increasing aliphatic chain length of diester. This further strengthens the higher crystallinity for gels

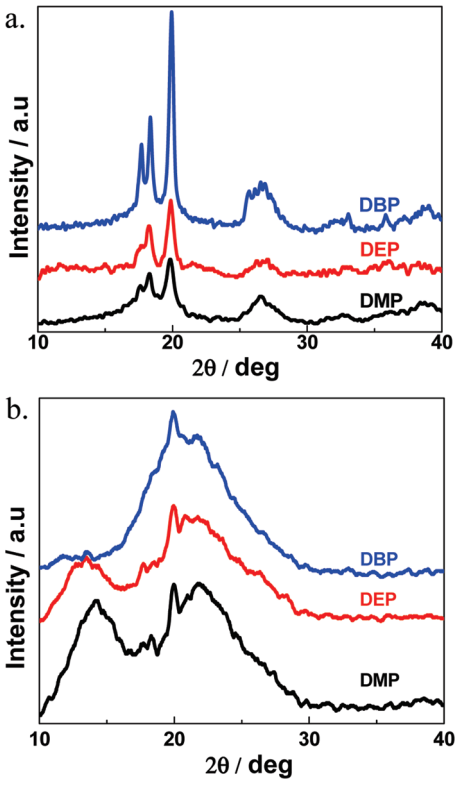

Figure 2. XRD patterns of CTFE (a) dried gels and (b) gels of indicated solvents.

with higher *n* phthalates. However, XRD observation confirms the crystalline structure in gel which provides the reason for three-dimensional networks through the formation of crystallites. The crystallites are acting as cross-linking points in the gels to form polymer−solvent complex in the presence of solvent molecules. FTIR spectra of CTFE dried gels in transmittance mode in the range of 400−1000 cm^{-1} are shown in Figure 3. The characteristic peaks of α-phase are observed at 489, 614, 763, and 976 cm^{-1}. The absorption band at 763 cm^{-1} is related to rocking vibration, and the band at 615 cm^{-1} is assigned to a mixed mode of CF_2 bending and C−C−C skeleton vibration.[37,38] The peak at 490 cm^{-1} band is related to bending and wagging vibrations ascribed to the α-polymorph. Moreover, there are two additional peaks at 510 and 840 cm^{-1}, indicating the presence of piezoelectric *β*-phase in dried gels which gets prominent for higher *n* phthalates, suggesting greater *β*-phase fraction for higher aliphatic chain length of diester. It is worthy to mention that pure PVDF do not exhibit any *β*-phase in gels while its copolymer with CTFE nucleates *β*-phase in same solvents (phthalates). The absence of *β* peak in XRD patterns indicates that the abundance of *β*-phase might be low in dried gel while the *β*-phase appears at ∼21° is merged with polymer−solvent complex peak for gels in the presence of solvent. The XRD peak for the compound formation and *β*-phase merge together at ∼21°, and thereby, it is difficult to get the particular phase content/compound formation. The *β*-peak is well-known at 21.2° while the exact location of the compound in not reported in the literature. However, FTIR studies indicate the existence of *β*-peak in gel. In this case, the XRD pattern provide us a clue while FTIR studies confirm the presence of *β*-phase.

Morphology. Surface morphologies of CTFE dried gels in two representative solvents (DMP and DBP) have been shown in Figure 4a. Fibrillar morphology is evident in both the phthalates and fibriller dimensions (diameter and length) decrease from dimethyl phthalate to dibutyl phthalate (Figure 4b). Fibrils are becoming thinner and shorter with increasing aliphatic chain length of phthalates like pure PVDF gels in the same series of solvents. So, it is assumed that more numbers of fibrils are required to from a cross-linked junction point in case of lower *n* phthalates because of poor interaction between polymers and solvent molecules while enhanced interaction with higher homologue of phthalates necessitate less number of fibrils to construct a junction point causing thinner fibrillar dimension.

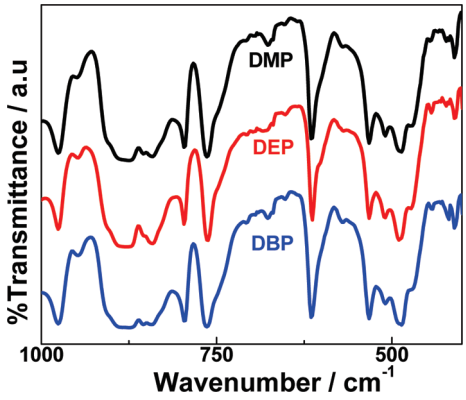

Figure 3. FTIR patterns of CTFE dried gels for indicated solvents.

Solvent Retention and Degradation. To understand the solvent retention power of the gels, TGA thermograms of CTFE gels (10 wt % polymer) in various phthalates are shown in Figure 5a. Weight loss starts at 165 °C and continued up to 90% weight loss in the first step, primarily due to loss of solvent from the gels. 5 wt % loss of solvent occurs at 167, 180, and 214 °C in DMP, DEP, and DBP solvent, respectively. So, it is clear that the solvent losses occur at higher temperature for higher homologue of phthalates. In other words, solvent retention power of gel increases with increasing aliphatic chain length of phthalates as the interactions between polymer chains and higher *n* phthalates are greater. Apart from the interactions between polymer and solvent, cohesive energy densities arising from the solvent−solvent and polymer−polymer interaction play an important role for the significant improvement in thermal properties of gels with higher homologues of phthalates.[43] Further, two-step degradation of the gels was recorded for all the solvents. The second degradation point at 447 °C is due to the copolymer (CTFE) decomposition, which is the same for all the gels. Figure 5b shows the DTA thermogram of CTFE gels in various phthalates. The larger endothermic peaks indicate the solvent evaporation from gels which are shifted to higher temperature for larger *n*. Moreover, there are small endotherms (shown in the inset) presumably due to gel melting, and it increase with aliphatic chain length of phthalates. The gel melting temperatures are 108, 114, and 137 °C in DMP, DEP, and DBP, respectively, showing the formation of compact and ordered crystallites with higher aliphatic chain length of phthalates. The associated heats of fusion from the respective peak area are 4.2. 4.9 and 5.7 J/g for DMP, DEP, and DBP, respectively, further exhibiting the formation of greater crystallites for higher *n* phthalates.

Gel Formation and Its Melting. The gel melting and cooling behaviors in various phthalates have been presented in Figure 6. Gel melting points are 98, 116, and 136 °C for gels with DMP, DEP, and DBP, respectively, showing clear increase of melting

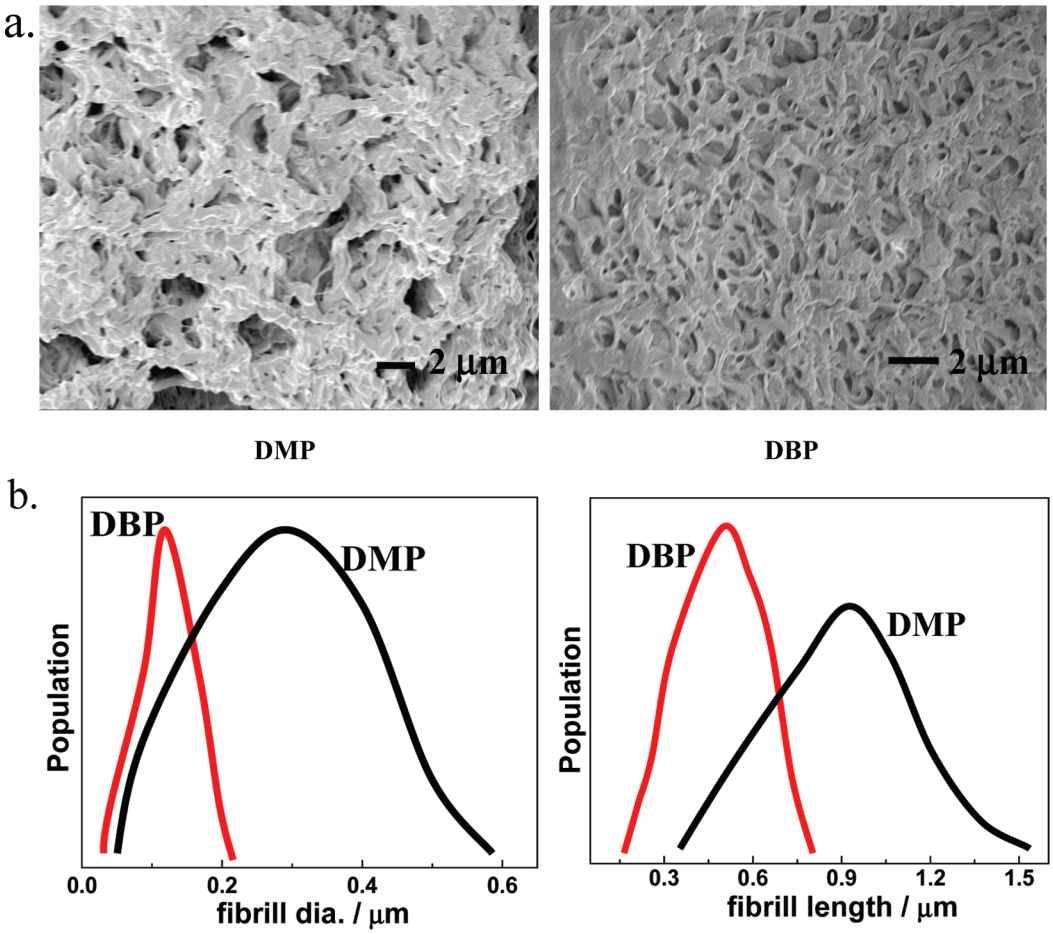

Figure 4. (a) SEM micrographs of CTFE gels (10% (w/v)) in indicated solvents. (b) Distribution of fibril diameter and length obtained in two solvents (polymer concentration was kept constant at 10% (w/v)).

temperature with increasing aliphatic chain length of phthalates. Both DTA and DSC experiments exhibit similar trend of gel melting due to compact and ordered crystallites formed in higher *n* phthalates. Further, the gelation temperatures, as observed from cooling curves, show higher values for higher aliphatic chain length phthalates indicating faster gelation for higher *n* phthalates. The gelation temperatures are 37, 42, and 78 °C in DMP, DEP, and DBP, respectively.[18,19] Double melting endotherms indicate the presence of two kinds of crystallites: low-temperature peak demonstrates the scattered and thinner crystallites embedded in amorphous zone while the organized thicker crystallites originate at the high-temperature peak. However, both the gelation and gel melting behavior are varied differently as a function of aliphatic chain length of phthalates, showing a diverse thermodynamic system.

Thermodynamics and Compound Formation. Figure 7a,b shows gel melting (T_m) and gelation temperature (T_{gel}) of CTFE gel in two representative solvents (DMP($n = 1$) and DBP($n - 4$)) as a function of polymer concentration (w_p) in gels. The upper curve corresponds to melting temperatures of the gel and lower curve correspond to gelation temperatures during cooling. Initially, both the T_m and T_{gel} increase with increasing polymer concentration and level off at the higher concentration. There is a significant decrease of T_m and T_{gel} observed at lower weight fraction of polymer for lower aliphatic chain length of phthalate (DMP) while that are only marginal in case of higher *n* phthalates (DBP). The greater interactions between the higher homologue of phthalates and polymer below $w_p < 0.45$ in contrast to weak interaction for lower homologue cause this behavior. This was auxiliary supplemented by the formation of weak gel in DMP and moderately strong gel in DBP at lower concentration of polymer ($w_p < 0.45$). Further, there is a pronounced difference between the melting and gelation temperatures (~30−35 °C) in each solvent. It might be due to the hysteresis effect of the first order transition. Figure 8 exhibits the compound formation of CTFE gels in dimethyl phthalate and dibutyl phthalate as calculated from heat of fusion of gels. All the heat of fusion values lie above the line connecting heat of fusion of pure CTFE and various solvents. The deviations from linearity indicate the formation of compounds of polymer solvents complexes. Moreover, two different peaks for heat of fusion of CTFE have been observed after carefully fitted the experimental data points for both the solvents, suggesting the formation of two different compounds. Heat of fusion of the compounds can be calculated using eq 1.

$$\Delta H - w_{PVDF}\Delta H_{PVDF} = \Delta H_{comp} \quad (1)$$

The ΔH of compound formed was measured from the total heat of enthalpy and heat of fusion of respective CTFE weight fraction. Figure 9 has shown the representative plot of ΔH_{comp} vs w_p for CTFE−DMP and CTFE−DBP systems. Two peaks confirm the existence of two different compounds with varying compositions for both the solvents. The composition of the

dx.doi.org/10.1021/ma200271j |*Macromolecules* 2011, 44, 3029–3038

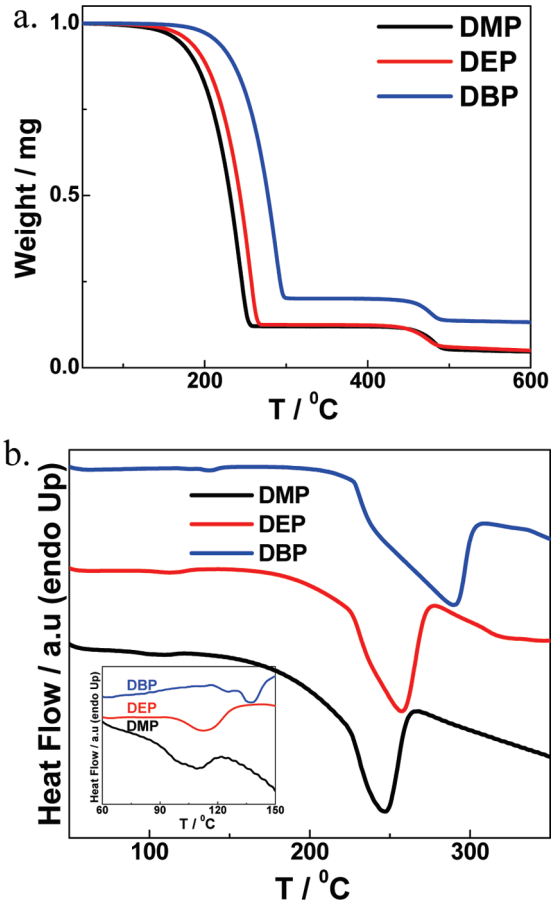

Figure 5. (a) TGA thermograms of the CTFE gels in indicated solvents. (b) DTA thermograms of the CTFE gels in indicated solvents.

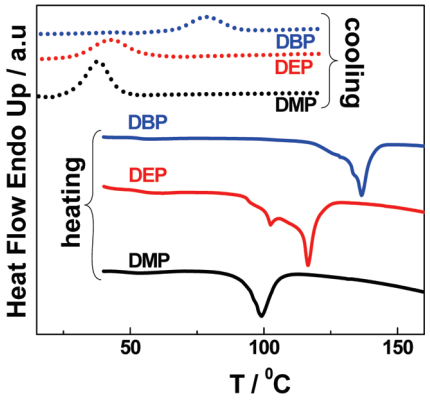

Figure 6. DSC thermograms (heating and cooling curves) of CTFE gels prepared in indicated phthalate solvents. The heating and cooling rate was kept at 10 °C min^{-1}.

compound formed gradually shifts to lower weight fraction of CTFE with increasing n. The values are 0.49 and 0.40 for lower composition peak and 0.71 and 0.68 for the higher composition peak for DMP and DBP, respectively. So, it is apparent that there is significant shift of lower composition peak while higher composition peak is having almost similar composition. The ratios of the monomeric units of CTFP and phthalate molecule are 6:1 and 4:1 for DMP and DBP, respectively, for the higher composition

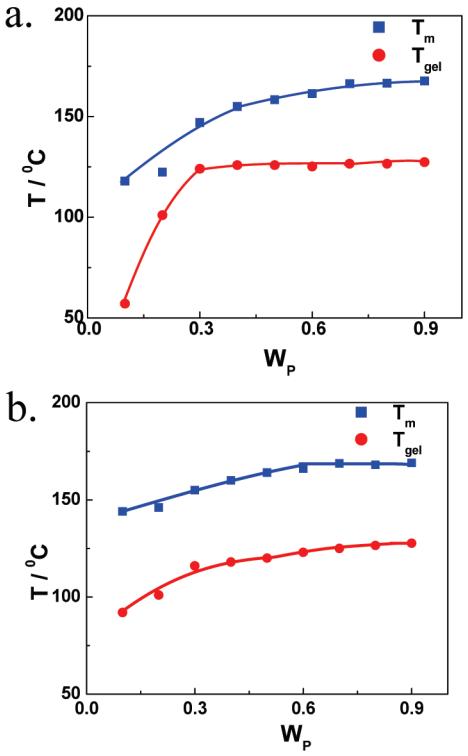

Figure 7. Gel melting and gelation temperature vs weight fraction of CTFE in gels (a) in DMP and (b) in DBP solvents.

peak ($w_p \sim 0.70$). In other words, every single phthalate molecule needs 6 and 4 monomeric units to form a complex with DMP and DBP, respectively. Moreover, for lower composition peak ($w_p = 0.40-0.49$) the ratio of the monomeric units of CTFP and phthalate molecule is constant at 3:2 for both the phthalates. However, two different compounds of copolymer in gels have been observed mainly due to the two different site of interactions of CTFE copolymer, i.e., $\rangle CF_2$ and $\rangle CF_2-CF(Cl)$ from two monomers with the $\rangle C{=}O$ groups of phthalates. Previously, we observed the strong interaction between pure PVDF/HFP copolymer with phthalates and found single compound for pure PVDF and two compounds for the copolymer.[19] We may conclude that copolymers are forming two compounds arising from two different interaction sites present in single polymer molecule (two separate monomer) while one type of interaction site provides only one compound formation in pure polymer.

Small-Angle Neutron Scattering. Small-angle neutron scattering patterns of dried gels prepared from DMP, DEP, and DBP solvents are shown in Figure 10 to provide insight of the fibrillar structure appearing through SEM images. Interestingly, a small hump appeared in SANS patterns, indicating the lamellar organization inside the fibrils. Moreover, the shoulder has shifted to higher q range with increasing aliphatic chain length of diesters. The characteristic lengths, $\Lambda_c = 2\pi/q_m$, are 8.7, 7.8, and 7.5 nm for DMP, DEP, and DBP, respectively, where q_m is the wavevector corresponding to the peak position. The interlamellar distance decreases slightly with increasing aliphatic chain length of diesters. The correlation lengths, ξ, have been calculated from lower q-range by using Debye−Bueche model (inset figure using eq 2). The ξ values are 16.0, 20.7, and 23.4 nm in DMP, DEP, and DBP, respectively, showing increasing tendency with increasing n. Hence, the crystallites, arising from the association of few

dx.doi.org/10.1021/ma200271j |Macromolecules 2011, 44, 3029–3038

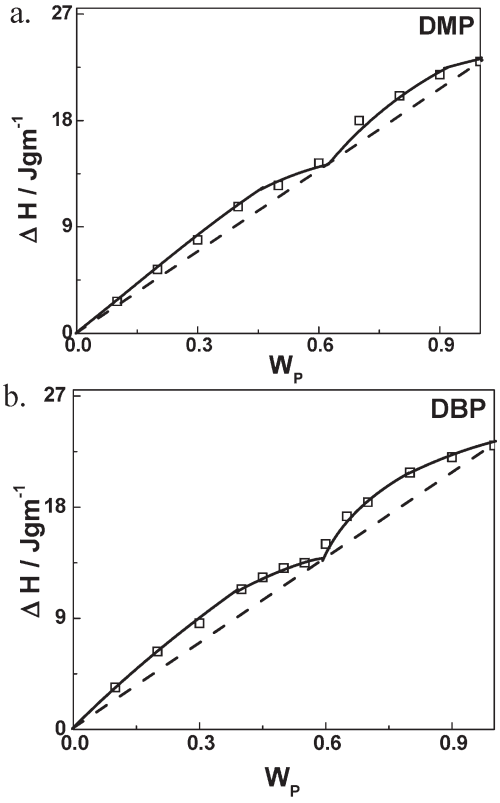

Figure 8. Plot of enthalpies vs weight fraction of CTFE during the gel melting process in indicated phthalate solvents.

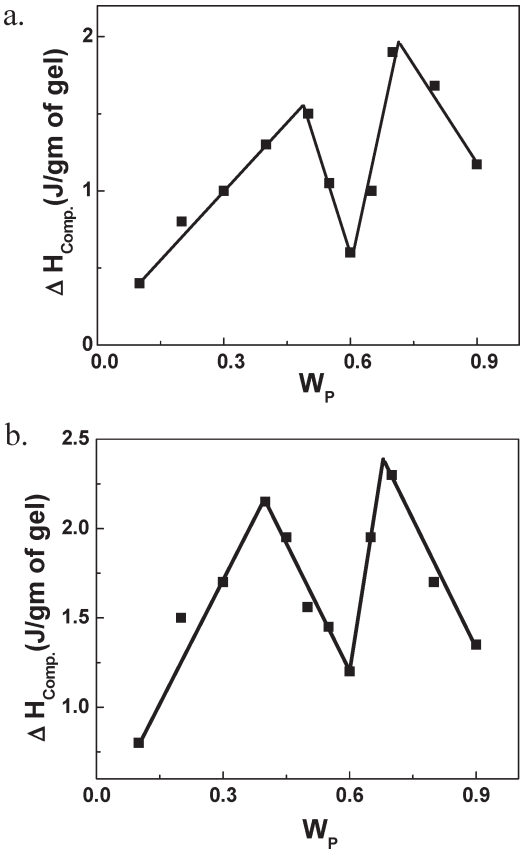

Figure 9. Representative plots for the heat of fusion of compounds (polymer−solvent complexes) vs weight fraction of CTFE in gels (a) DMP and (b) DBP solvents.

lamellae, dimension increases with increasing n. SANS studies provide insight on lamellar structure of fibril and the correlation length of gels prepared from various phthalates. However, the characteristic length decreases while the correction length increases with increasing aliphatic chain length, suggesting gelation is easier for higher homologues of aliphatic chain length of diesters.

$$I(q) = \frac{I(0)}{(1 + \xi^2 q^2)^2} \qquad (2)$$

Small-Angle X-ray Scattering. The SAXS profiles of the dried gels plotted on log−log scale have been presented in Figure 11. The SAXS profiles follow a linear power-law behavior of the form $I(q) \sim q^{-\gamma}$ over a wider q range with noninteger values for γ. This power-law intensity arises from the concentrated regions having a fractal nature for their morphology. The values of the exponent γ vary from 2.80 to 3.05 to 3.7 for DMP, DEP, and DBP, respectively. Thus, in DMP, the concentrated dense regions or clusters form as mass fractal with dimension 2.8. This morphology gradually transforms to surface fractal nature with fractal dimension ($D_s = 6 - \gamma$) from DEP ($D_s = 2.95$) to DBP ($D_s = 2.3$). This suggests a rough surface of the clusters with comparatively more smoother surfaces in case of DBP. The samples are known to have condensed and low-density regions formed as a result of phase separation during the onset of gelation. Further, crystallites or cross-link points are formed in the host matrix in the concentrated mass regions. Moreover, there are shoulders in all the SAXS profile, and the peak position of the shoulder gradually shifted to higher q region with increasing aliphatic chain length of diesters. These humps are also indicative

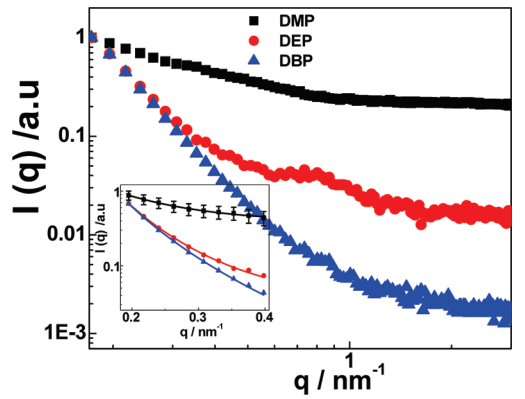

Figure 10. Small-angle neutron scattering intensity $I(q)$ of CTFE gels prepared from indicated solvents. The solid lines in the inset figure represent the Debye−Bueche fitting at lower wavevector region. The error bar has been shown only for DMP to avoid clumsiness in data for DEP and DBP.

of lamellar organization within the fibibrillar morphology, as observed in SANS studies. Hence, both the SANS and SAXS studies suggest the lamellar patterns which further self-assembled to form thicker fibril observed in SEM micrographs.

Molecular Modeling. It is clear from the phase diagram that CTFE copolymer and phthalates form two different types of polymer−solvent complexes with varying compositions. In order

dx.doi.org/10.1021/ma200271j |*Macromolecules* 2011, 44, 3029–3038

to model the complexes, a semiempirical AM1 (electronic structure calculations) method has been used. Initially, both the structure of CTFE copolymer and diester were energetically minimized. The phthalates and CTFE molecules can move toward each other to form complex either in cis or trans conformation as the energy difference between the two is small and conformational transformation may occur during geometry optimization. It is presumed that the interacting sites of CTFE and diester are the $\rangle CF_2$, $\rangle C^*F_2CF(Cl)$, and $\rangle C{=}O$ moieties, respectively, through which dipole−dipole type of interactions may exist due to electronic polarization. Figure 12a,b shows the representative energy-minimized complexes in DMP and DBP using the double strand of CTFE truncated chain and respective phthalates. The dashed lines show the distances between the two nearest interacting sites for two $\rangle C{=}O$ groups and $\rangle CF_2$ groups from two separate strands of CTFE. Two carbonyl groups interact with the $\rangle CF_2$ group from two opposite sides of the solvent through dipole−dipole interaction, suggesting two types complex formation in gels. The dipole−dipole distances have been calculated for the whole series of phthalates up to $n = 9$ and are presented in Figure 13. Interestingly, both the dipolar distances gradually decrease up to $n = 6$, suggesting greater interaction and subsequently increases with further increase of aliphatic chain length of diester. The initial decrease of dipolar distance can explain well the higher gelation rate for higher n phthalates, and the larger distances after $n = 6$ explain why CTFE cannot form gel in dioctyl phthalates ($n = 8$). So, the electronic structure calculation predicts nicely both the relative rate of gelation and the reason for not forming gel after certain aliphatic chain length ($n = 6$) of the diester. In conclusion, the molecular modeling suggests that in the case of trans

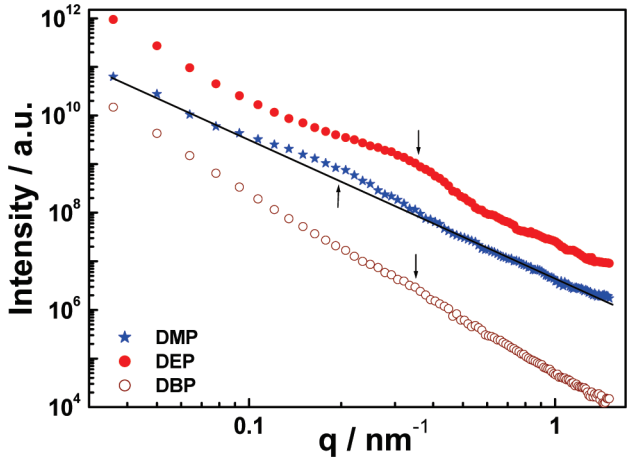

Figure 11. Small-angle X-ray scattering intensity $I(q)$ of CTFE dried gels prepared from indicated solvents. The arrows show the peak position of the shoulders.

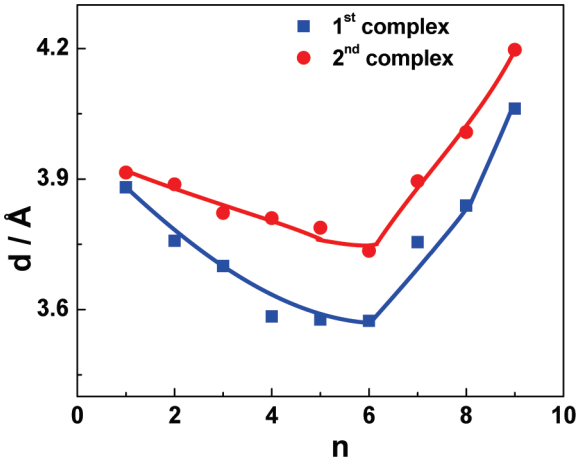

Figure 13. Two shorter distances between two interactive dipoles in two different CTFE strands in CTFE-phthalate complexes in, shown above as a function of aliphatic chain length (n) considering double-stranded models. The solid lines are arbitrarily drawn to show the nature of changes.

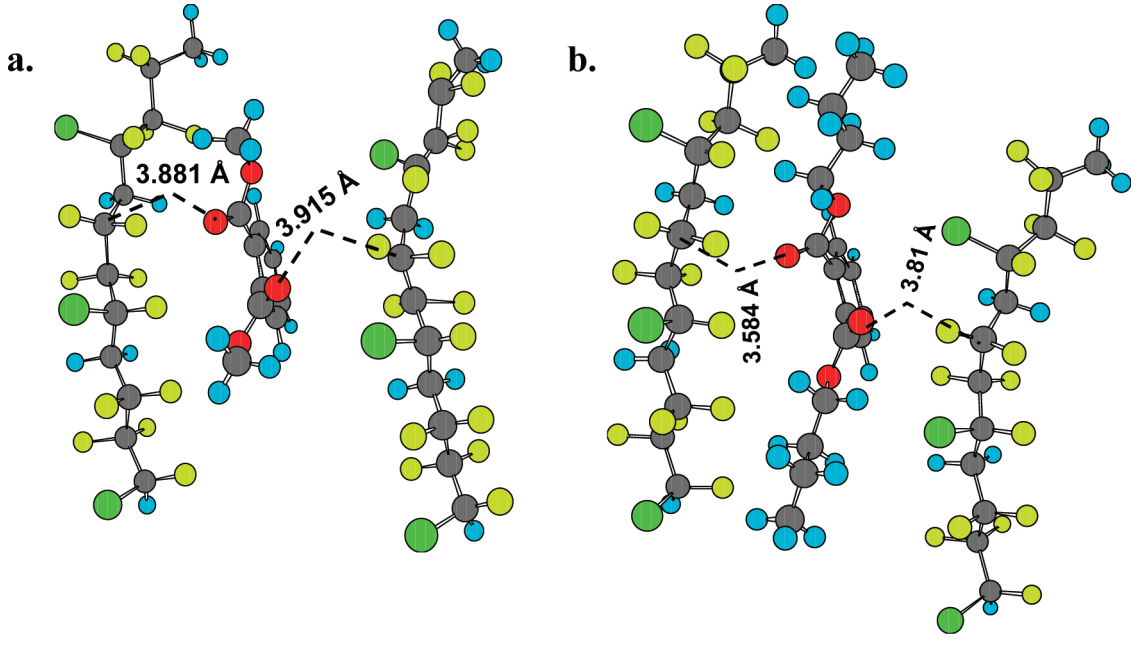

Figure 12. Molecular models of CTFE-phthalate complexes obtained from energy-minimized electronic structure calculation (a) in DMP and (b) in DBP solvent showing the distances between two nearest dipoles on both sides of the solvent.

dx.doi.org/10.1021/ma200271j |*Macromolecules* 2011, 44, 3029–3038

Scheme 2. Schematic Representation of Self-Assembly (Bottom-up Approach) Starting from Molecular Compound (Polymer−Solvent Complex), Lamellar Organization Leading to Construction of Individual Fibril

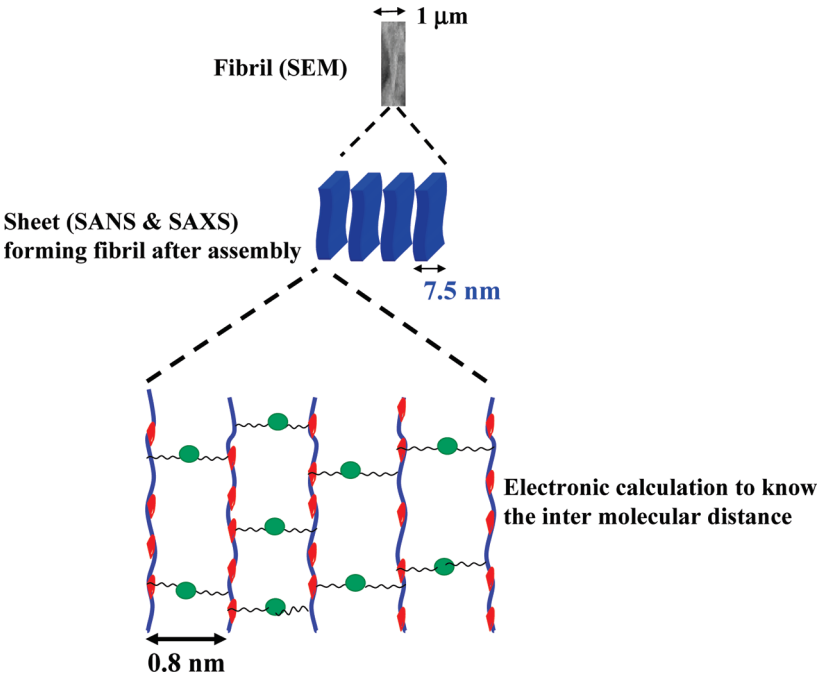

form minimum distance of approach of phthalates toward CTFE chain initially decreases with chain length of the diester group of phthalate and then increases for $n > 6$, passing through a minimum for C_6 carbon chain length in CTFE copolymer that strongly supports the experimental observations. In addition, the modeling and thermodynamics of compound formation correspond to each other, and we can assign the composition of the complexes from the dipolar distances in energy-minimized state.

It is evident that phthalate molecules interact with two neighboring CTFE strands through its two carbonyl groups with $\rangle CF_2$ units of polymer chains. We predict a bottom-up approach for the whole gelation process (Scheme 2) where molecular level interaction envisage two polymer chains laying apart with a distance of 0.80 nm (as calculated by the electronic structure calculation) and strongly held up by the two interacting sites of the phthalates in two opposite directions. Few of such assemblies are connected together to form a lamellae structure, and the average distance between the lamella is measured by using SANS as ~7.5 nm. It is needless to mention that few of the lamellar assemblies construct the fibril as observed in SEM micrograph. The self-assembly via the formation of molecular compound, and, thereby, the congregation of lamellar organization to construct a fibril, observable in SEM, is presented in Scheme 2.

Another observation we have made that six is a critical number of aliphatic chain carbon below which phthalates form gels and above which it cannot form gel with CTFE copolymer, and previously we have observed that this phenomenon is true for pure PVDF and another copolymer of hexafluoropropylene. In order to investigate the reason behind the magic number of six, we have computed charge separation of ⟩C═O group of phthalate molecules with varying chain length of the substituted group. Our calculations reveal that the charge separation increases initially with increase in number of aliphatic chain carbon up to

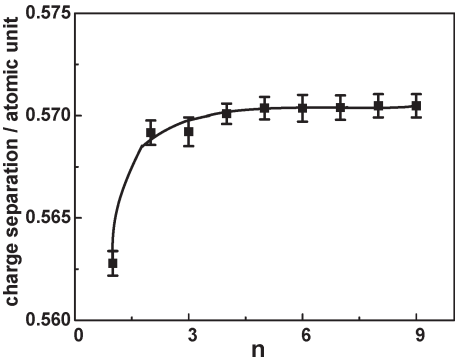

Figure 14. Mülliken charge separation (in atomic unit) of ⟩C═O as a function of the number of aliphatic chain carbon.

$n = 6$ as depicted by Figure 14 and then levels off. This can be anticipated from the fact that up to $n = 6$ the positive inductive effect of the substituted alkyl group is appreciable, and beyond that it is insignificant due to longer distance inductive effect which practically remains same irrespective of the chain length. On the other hand, our electronic structure calculation of binding between CTFE and phthalate molecules indicates that their closest approach (as shown in Figure 12) gets highly sterically hindered beyond $n = 6$ as depicted in Figure 13 (from the closest distance of approach vs n plot). One would, therefore, expect that the gelation of diesters with CTFE is going to take place with phthalate molecules up to a chain length with $n = 6$.

CONCLUSION

Thermoreversible gelation of poly(vinylidene fluoride-*co*-chlorotrifluoroethylene) copolymer in phthalates with varying

dx.doi.org/10.1021/ma200271j |*Macromolecules* 2011, 44, 3029–3038

aliphatic chain length has been reported. Gelation rate increases with increasing aliphatic chain length. The structure has been illustrated through XRD and FTIR studies, indicating the formation of compound and some extent of β-phase in gels. Solvent retention power of gels increases with increasing n, indicating the stronger interaction between the copolymer and solvent at higher aliphatic chain length while the thermal degradation of copolymer occurs at same temperature in absence of any solvent. The plots of enthalpy vs copolymer composition show a positive deviation from linearity, suggesting the formation of compound and the two peaks confirm the creation of two compounds with different compositions. The detailed structure of the crystallite have been observed through SANS and SAXS measurement revealing lamellar organization. Molecular modeling through energy minimization program explains the relative rate of gelation with varying aliphatic chain length and complex formation in gels. It turns out from our electronic structure calculations that charge separation gradually favors gelation up to aliphatic chain carbon number six. The steric hindrance of aliphatic chain length for binding between phthalate and polymer unit, on the other hand, is highly dominating beyond aliphatic chain carbon number six. This justifies the critical number of aliphatic chain carbon six up to which phthalates form gels with CTFE copolymer.

AUTHOR INFORMATION

Corresponding Author
*E-mail: pmaiti.mst@itbhu.ac.in.

ACKNOWLEDGMENT

P. Jaya Prakash Yadav acknowledges the council of scientific and industrial research for granting a Senior Research fellowship. The supply of polymer and copolymer samples from Ausimont, Italy, is gratefully acknowledged. Authors also acknowledge Dr. D. K. Avasthi and Mr. Pawan K. Kulriya of IUAC, New Delhi, for XRD measurements.

REFERENCES

(1) Scrosati, B. *Chim. Ind.* **1997**, *79*, 463.
(2) Choe, H. S.; Carroll, B. G.; Pasquariello, D. M.; Abraham, K. M. *Chem. Mater.* **1997**, *9*, 369.
(3) Appetecchi, G. B.; Scrosati, B. *Electrochim. Acta* **1998**, *43*, 115.
(4) Tazaki, M.; Wada, R.; Okabe, M.; Homma, T. *J. Appl. Polym. Sci.* **1997**, *65*, 1517.
(5) Hasegawa, R.; Kobayashi, M.; Tadokoro, H. *Polym. J.* **1972**, *3*, 593.
(6) Hasegawa, R.; Takahashi, Y.; Chatani, Y.; Tadokoro, H. *Polym. J.* **1972**, *3*, 600.
(7) Lando, J. B.; Olf, H. G.; Peterlin, A. *J. Polym. Sci., Part A-1* **1969**, *4*, 941.
(8) Kobayashi, M.; Tashiro, K.; Tadokoro, H. *Macromolecules* **1975**, *8*, 158.
(9) Basset, D. C. In *Development in Crystalline Polymers*; Basset, D. C., Ed.; Applied Science Publishers: London, 1982.
(10) Cho, J. W.; Song, H. Y.; Kim, S. Y. *Polymer* **1993**, *34*, 1024.
(11) Mal, S.; Maiti, P.; Nandi, A. K. *Macromolecules* **1995**, *28*, 2371.
(12) Mal, S.; Nandi, A. K. *Polymer* **1998**, *30*, 6301.
(13) Dasgupta, D.; Nandi, A. K. *Macromolecules* **2005**, *38*, 6504.
(14) Dasgupta, D.; Manna, S.; Malik, S.; Rochas, C.; Guenet, J. M.; Nandi, A. K. *Macromolecules* **2005**, *38*, 5602.
(15) Dikshit, A. K.; Nandi, A. K. *Langmuir* **2001**, *17*, 3607.
(16) Dikshit, A. K.; Nandi, A. K. *Macromolecules* **2000**, *33*, 2616.
(17) Yadav, P. J. P.; Ghosh, G.; Maiti, B.; Aswal, V. K.; Goyal, P. S.; Maiti, P. *J. Phys. Chem. B* **2008**, *112* (15), 4594.
(18) Yadav, P. J. P.; Patra, A. K.; Sastry, P. U.; Ghorai, B. K.; Maiti., P. *J. Phys. Chem. B* **2010**, *114*, 11420.
(19) Yadav, P. J. P.; Aswal, V. K.; Sastry., P. U.; Patra., A. K.; Maiti., P. *J. Phys. Chem. B* **2009**, *113*, 13516.
(20) Tazaki, M.; Wada, R.; Okabe, M.; Homma, T. *J. Appl. Polym. Sci.* **1998**, *65*, 1517.
(21) Malik, S.; Rochas., C.; Schmutz, M.; Guenet, J. M. *Macromolecules* **2005**, *38*, 6024.
(22) Malik, S.; Rochas., C.; Guenet, J. M. *Macromolecules* **2005**, *38*, 4888.
(23) Ray, B.; Elhasri, S.; Thierry, A.; Marie, P.; Guenet, J. M. *Macromolecules* **2002**, *35*, 9730.
(24) Dixit, A. K.; Jana., T.; Malik, S.; Nandi, A. K. *Polym. Int.* **2003**, *52*, 925.
(25) Zhou, Y.; Yang, D.; Gao, X.; Chen, X.; Xu, X.; Xu, Q.; Lu, F.; Nie, J. *Carbohydr. Polym.* **2009**, *75*, 293.
(26) Kanaya, T.; Ohkura, M.; Kaji, K.; Furusaka, M.; Misawa, M. *Macromolecules* **1994**, *27*, 5609.
(27) Takcshita., H.; Kanaya, T.; Nishida, K.; Kaji, K.; Takahashi, T.; Hashimoto, M. *Phys. Rev. E* **2000**, *61*, 2125.
(28) Kanaya, T.; Ohkura, M.; Takeshita, H.; Kaji, K.; Furusaka, M.; Yamaoka, H.; Wignal, G. D. *Macromolecules* **1995**, *28*, 3168.
(29) Higgins, J. S.; Benoit, H. C. *Polymers and Neutron Scattering*; Clarendon Press: Oxford, 1994.
(30) Schmidt, P. W.; Anvir, D.; Levy, D.; Hohr, A.; Steiner, M.; Röll, A. *J. Chem. Phys.* **1991**, *94*, 1474.
(31) Schmidt, P. W.; Height, R. *Acta Crystallogr.* **1960**, *13*, 480.
(32) Schmidt, P. W. *J. Appl. Crystallogr.* **1991**, *24*, 414.
(33) Kobayashi, M.; Tashiro, K.; Tadokoro, H. *Macromolecules* **1975**, *8*, 158.
(34) Ramzi., M.; Rochas., C.; Guenet, J. M. *Macromolecules* **1996**, *29*, 4668.
(35) Guenet, J. M. *Thermochim. Acta* **1996**, *284*, 67.
(36) Malik, S.; Nandi, A. K. *J. Phys. Chem. B* **2004**, *108*, 597.
(37) Manna, S.; Batabyal, S. K.; Nandi, A. K. *J. Phys. Chem. B* **2006**, *110*, 12318.
(38) Dasgupta, D.; Malik, S.; Thierry, A.; Guenet, J. M.; Nandi, A. K. *Macromolecules* **2006**, *39*, 6110.
(39) Frisch, M. J.; Trucks, G. W.; Schlegel, H. B. *GAUSSIAN 03, Revision E.01*, Gaussian Inc.: Wallingford, CT, 2007.
(40) Adem, E.; Rickards, J.; Burillo, G.; Avalos-Borja, M. *Radiat. Phys. Chem.* **1999**, *54*, 637.
(41) Tashiro, K.; Tadokoro, H.; Kobayashi, M. *Ferroelectrics* **1981**, *32*, 167.
(42) Hasegawa, R.; Takahashi, Y.; Chatani, Y.; Tadokoro, H. *Polym. J.* **1972**, *3* (5), 600.
(43) Marchetti, M.; Prager, S.; Cussler, E. L. *Macromolecules* **1990**, *23*, 3445.